Bone 47 (2010) 591–597

Contents lists available at ScienceDirect

Bone

journal homepage: www.elsevier.com/locate/bone

Skeletal phenotype of mandibuloacral dysplasia associated with mutations in *ZMPSTE24*

Vicki J. Cunningham [a,*], Maria Rosaria D'Apice [b], Norma Licata [c], Giuseppe Novelli [b,d], Tim Cundy [e]

[a] Child Health Centre, Northland District Health Board, New Zealand
[b] Department of Biopathology and Diagnostic Imaging, Tor Vergata University, Rome, Italy
[c] IRCCS Centro Neurolesi "Bonino-Pulejo", Messina, Italy
[d] Ospedale San Pietro Fatebenefratelli, Rome, Italy
[e] Department of Medicine, Faculty of Medical & Health Sciences, University of Auckland, New Zealand

ARTICLE INFO

Article history:
Received 29 March 2010
Revised 3 June 2010
Accepted 5 June 2010
Available online 13 June 2010

Edited by: S. Ralston

Keywords:
Mandibuloacral dysplasia
ZMPSTE24
LMNA
Bisphosphonate
Skeletal phenotype

ABSTRACT

Mandibuloacral dysplasia (MAD) is a rare recessively inherited premature aging disease characterized by skeletal and metabolic anomalies. It is part of the spectrum of diseases called laminopathies and results from mutations in genes regulating the synthesis of the nuclear laminar protein, lamin A. Homozygous or compound heterozygous mutations in the *LMNA* gene, which encodes both the precursor protein prelamin A and lamin C, are the commonest cause of MAD type A. In a few cases of MAD type B, mutations have been identified in the *ZMPSTE24* gene encoding a zinc metalloproteinase important in the post-translational modification of lamin A. Here we describe a new case of MAD resulting from compound heterozygote mutations in *ZMPSTE24* (p.N256S/p.Y70fs). The patient had typical skeletal changes of MAD, but in addition a number of unusual skeletal features including neonatal tooth eruption, amorphous calcific deposits, submetaphyseal erosions, vertebral beaking, severe cortical osteoporosis and delayed fracture healing. Treatment with conventional doses of pamidronate improved estimated volumetric bone density in the spine but did not arrest cortical bone loss. We reviewed the literature on cases of MAD associated with proven *LMNA* and *ZMPSTE24* mutations and found that the unusual features described above were all substantially more prevalent in patients with mutations in *ZMPSTE24* than in those with *LMNA* mutations. We conclude that MAD associated with *ZMPSTE24* mutations has a more severe phenotype than that associated with *LMNA* mutations—probably reflecting the greater retention of unprocessed farnesylated prelamin A in the nucleus, which is toxic to cells.

Introduction

The progeroid syndromes are rare genetic disorders with shared characteristics of premature aging. There are important phenotypic differences between the various syndromes, but most have skeletal features that may include osteoporosis and fractures [1–12, Table 1]. One of the progeroid syndromes, mandibuloacral dysplasia (MAD), which results from abnormalities in the nuclear laminar proteins, lamins A and C, has a highly distinctive skeletal phenotype, including mandibular and clavicular hypoplasia, dental crowding and erosion of the terminal phalanges. In addition, MAD patients develop skin anomalies, lipodystrophy and metabolic complications. The most frequently encountered form of MAD (MADA; OMIM 248370) is characterized by type A lipodystrophy with partial loss of subcutaneous fat from the extremities and excess fat deposition in the neck and trunk. MADA arises from mutations in the *LMNA* gene, which encodes the precursor protein prelamin A and lamin C [13]. To form the mature lamin A protein, prelamin A must undergo post-translational modification—a process that includes cleavage of peptides from its C-terminal end by the zinc metalloproteinase ZMPSTE24. MAD patients with more generalized loss of subcutaneous fat (type B lipodystrophy) (MADB; OMIM 608612) have been shown to have mutations in the *ZMPSTE24* gene that encodes this enzyme [14–16].

We describe in this paper the sixth published case of MAD associated with *ZMPSTE24* mutations. In addition to the usual skeletal phenotype, the patient concerned had a number of unusual skeletal features. Our review of the literature suggests these skeletal features are relatively specific for *ZMPSTE24* mutations. Our patient has type A lipodystrophy unlike the other cases of MAD with *ZMPSTE24* mutations.

Materials and methods

The blood samples from the affected patient and his parents were collected after informed consent was approved. Genomic DNA was

* Corresponding author. Child Health Centre, Private Bag 9742, Whangarei 0148, New Zealand. Fax: +64 9 430 4130.
E-mail address: Vicki.Cunningham@northlanddhb.org.nz (V.J. Cunningham).

8756-3282/$ – see front matter © 2010 Elsevier Inc. All rights reserved.
doi:10.1016/j.bone.2010.06.004

Table 1
Molecular basis and skeletal phenotype of progeroid syndromes.

Syndrome	OMIM	Inheritance	Gene	Skeletal phenotype	Reference
DNA repair defects					
Werner	277700	AR	*RECQL2*	Short stature, subcutaneous calcification, osteosarcoma, insufficiency fractures, non-union, dystrophic teeth	[1,2]
Bloom	210900	AR	*RECQL3*	Short stature, dystrophic teeth, osteosarcoma	[3]
Rothmund–Thomson	268400	AR	*RECQL4*	Short stature, upper limb (radial) defects, osteosarcoma metaphyseal trabeculation, brachymesophalangy, thumb hypoplasia, osteopenia, dystrophic teeth	[4]
Cockayne	216400	AR	*ERCC6*	Short stature (truncal shortening>limb), flexion contractures, facial dysmorphism	[5]
Xeroderma pigmentosa with progeroid features	610965	AR	*ERCC4*	Short stature, bird-like facies, microcephaly, scoliosis	[6]
Trichothiodystrophy	601675	AR	*ERCC3*		
ERCC2	Short stature, axial osteosclerosis, appendicular osteopenia, joint contractures	7.			
Golgi defect					
Geroderma osteodysplastica	231070	AR	*GORAB*	Kyphoscoliosis, osteopenia, vertebral fractures, Wormian bones, hip dislocation	[8]
Other					
Cutis laxa with progeroid features	612940	AR	*PYCR1*	Intrauterine growth restriction, facial dysmorphism, joint dislocation, osteoporosis, Wormian bones	[9]
Hallermann–Streiff	234100	AR	*?*	Brachycephaly with frontal bossing, micrognathia, dental anomalies, proportionate short stature	[10]
Wiedemann–Rautenstrauch	264090	AR	*?*	Short stature, macrocephaly, facial hypoplasia, narrow long bones with wide metaphyses	[11]
Lamin A defects					
Hutchinson–Gilford	176670	AD	*LMNA*	Short stature, micrognathia, coxa valga, acro-osteolysis, clavicular resorption	[12]
Mandibuloacral dysplasia A	248370	AR	*LMNA*	Short stature, mandibular hypoplasia, dental crowding, stiff joints, acro-osteolysis	[13]
Mandibuloacral dysplasia B	608612	AR	*ZMPSTE24*		[14]

extracted using automated extractor BIO ROBOT EZ1 and Qiagen EZ1 DNA Blood 350 µl kit (Qiagen, Chatsworth, CA). Proband's father genomic DNA was isolated also from hair roots, sperm and sputum. iQ kit (Promega, Madison, WI) was used for the extraction of the first two samples and oragene kit (DNA genotek, Ontario, Canada) for the third one. All extractions were performed in accordance with the manufacturer's protocol.

Molecular analysis of the *LMNA* gene was performed with LMNA gene amplification kit for direct sequencing (Diatheva s.r.l., Italy). *ZMPSTE24* amplification was carried out using published conditions [14]. The PCR products were purified and sequenced on ABI Prism 3130 (Applied Biosystems, Foster City, CA).

Genomic DNA extracted from sputum, hair roots and sperm of the patient's father was analyzed by pyrosequencing and real-time PCR techniques. Amplification of paternal and patient-derived genomic DNA was carried out according to standard PCR protocols using 5′ biotinylated forward primer 5′-GGCAAGCTATAAACCATTCG-3′ and reverse primer 5′-AGGTTAAGAAAGCATTCTGGG-3′. Biotinylated PCR product was incubated with the detection primer 5′-TTGAGAAATCTCGA-3′ designed with its 3′ end immediately upstream of the mutation. Pyrosequencing was carried out according to manufacturer's standard protocols (PyroSequencing AB, Uppsala, Sweden). To confirm pyrosequencing data, a more accurate analysis by real-time PCR was performed using Assays-by-Design for SNP Genotyping (Applied Biosystems). The reaction was performed in a volume of 25 µl with 10 ng of genomic DNA, 12,5 µl of TaqMan® Universal Master mix (Applied Biosystems) and 40× Assay Mix containing unlabeled PCR primers (ZMPFw 5′-CGGAGTTAGGACAGATCATGGATTC-3′, ZMPRv 5′-TCCTGACCAGAAGCTGAAAGTG-3′) and TaqMan® MGB probes (FAM-5′-AGAAATCTCGACTATCAAC-3′ to genotype the mutated ZMPSTE24 allele-specific, VIC-5′-AGAAATCTCGACTCTATCAAC-3′) to score the wild-type sequence. The thermal cycling conditions were 2′ at 50 °C, 10′ at 95 °C and 15″ at 95 °C and 1′ at 60 °C for 40 cycles.

Bone mineral density (BMD) measurements at the lumbar spine were made by dual energy x-ray densitometry (Lunar Prodigy, GE Healthcare, Little Chalfont, UK). Areal BMD is reported as the *z*-score. Estimated volumetric density was calculated as areal BMD/√projectional area at the third lumbar vertebra [17]. Combined cortical thickness at the mid-point of the tibia and femur was measured using a micrometer and the results compared to published normal values [18].

Consent was obtained from the patient and family to include clinical photographs.

Case report and results

The patient is the youngest of 4 children born to non-consanguineous parents of European origin. He was born prematurely at 33 weeks gestation with a birth weight of 2.51 kg (90th centile) and a head circumference of 32 cm (50th centile). Two teeth were already erupted at birth. During infancy, he had feeding problems relating to his small jaw, and by age 8 months both his height and weight were below the 3rd centile. He has sparse coarse hair, patchy alopecia, multiple lentigines, atrophic skin, a small beaked nose, scleroderma-like skin over the face, dermal calcinosis and dental crowding. He has lipodystrophy with very little subcutaneous fat over the limbs but with a prominent fat pad over his neck and cheeks (confirmed on CT scan) and a protuberant abdomen, consistent with Type A lipodystrophy (Fig. 1). In an effort to limit acral bone resorption, the patient was treated with intravenous pamidronate infusions (3 mg/kg/4 monthly, each treatment given as 4-h infusions over 3 consecutive days) between the ages of 4½ and 8½years. This treatment was well tolerated. Bone mineral density measurements of the lumbar spine were made annually during this period and thereafter at two yearly intervals.

Fig. 1. Photographs of the patient aged 13 years show downward sloping shoulders due to clavicular hypoplasia, sparse coarse hair, small beaked nose, micrognathia, protuberant abdomen and fat pad in anterior neck with absence of subcutaneous fat on the limbs (type A lipodystrophy), multiple lentigines on abdomen, ulcerated dermal calcinosis on left lateral thigh, fixed flexion contractures at the knees and bowed, shortened left humerus.

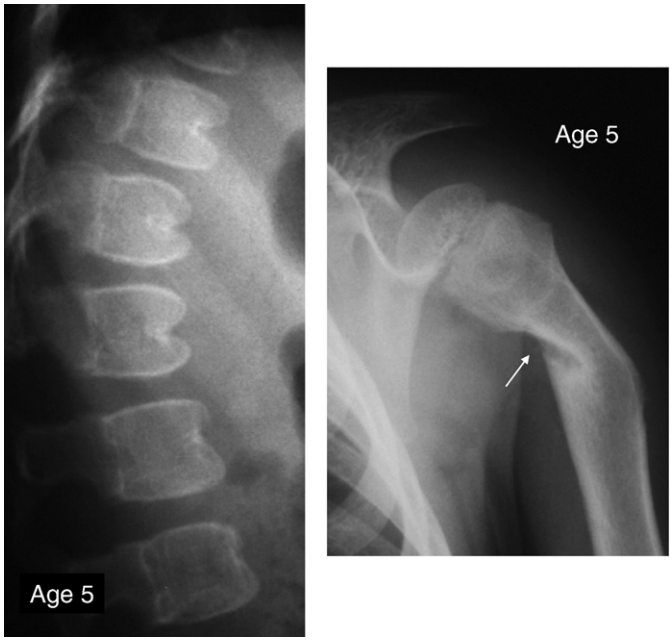

Fig. 3. Left: "Beaking" of the lower thoracic and upper lumbar vertebrae. Right: The curious submetaphyseal appearance and angulation in the proximal humerus (arrowed) was first noted on radiographs at the age of 3 years and was initially thought to represent a fracture. However, there was no pain and the changes were bilateral.

At the age of 11 years, he was noted to have hepatomegaly and elevated liver transaminases consistent with non-alcoholic steatohepatitis. At the age of 13 years, he developed type 2 diabetes, proteinuria (0.28 g/d) with normal renal function and ultrasound imaging and severe obstructive sleep apnoea (OSA) with upper airway obstruction—attributed to micrognathia. He entered puberty at 13 years of age, and by the age of 15 years he had progressed normally through puberty, his height standard deviation score was −3.2 and his BMI 17.7. At the age of 16 years, he now has limited independent mobility using crutches and relies on an electric wheelchair. He has normal intellect.

Skeletal phenotype

The skull showed typical features of MAD with mandibular hypoplasia with dental crowding and failure of fusion of the anterior mandibular rami. Unusual findings at birth were the presence of two erupted teeth and the failure of ossification of the occipital bone. Radiographs at the age of 8 months showed acral bone resorption in the terminal phalanges and clavicles. At the age of 4 years, radiographs showed that neither clavicle was visible but amorphous calcific masses were present in their place, which persisted into adolescence (Fig. 2). There was marked anterior "beaking" of the lower thoracic and upper lumbar vertebrae (Fig. 3). Symmetrical erosions of the proximal submetaphyseal regions of long bones with the formation of amorphous calcific masses were noted in the humeri, tibiae and femora (age 3 years) and the radii (age 6 years) (Figs. 3–5). These changes were progressive, particularly at the radii (Fig. 4). The patient sustained femoral fractures at age 8 and 13 years, and a tibial fracture at age 12 years (Fig. 5). The fractures were very slow to heal (>1 year). Obvious loss of cortical thickness in the long bones was noted between the ages of 3 and 14 years, at a time when cortical thickness should have been increasing (Figs. 5 and 6).

Serum calcium, phosphate and alkaline phosphatase levels were normal for age. Parathyroid hormone levels tended to be low (0.7–1.6 pmol/L). Markers of bone turnover (urinary N telopeptide and hydroxyproline) measured during pamidronate treatment period were in the appropriate range for the patient's age.

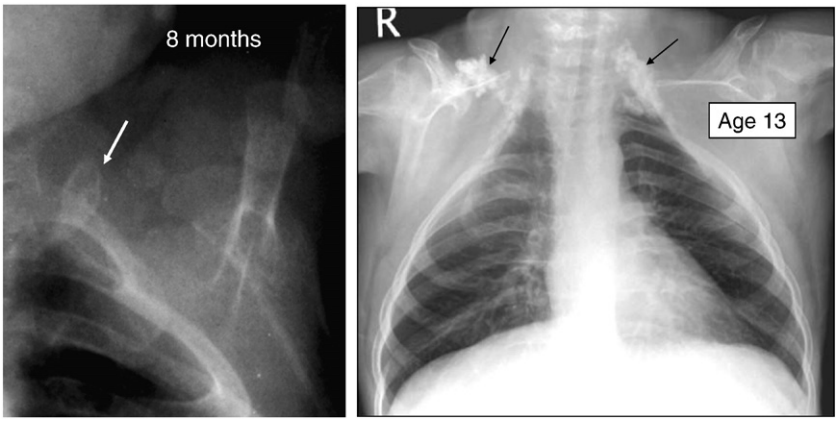

Fig. 2. Left: The clavicles were present on neonatal films, but by 8 months of age only a remnant of the clavicle persisted (arrowed). Neither clavicle was visible after the age of 4 years. Right: On the chest, radiograph bilateral amorphous calcific masses (arrowed) are present in place of the missing clavicles.

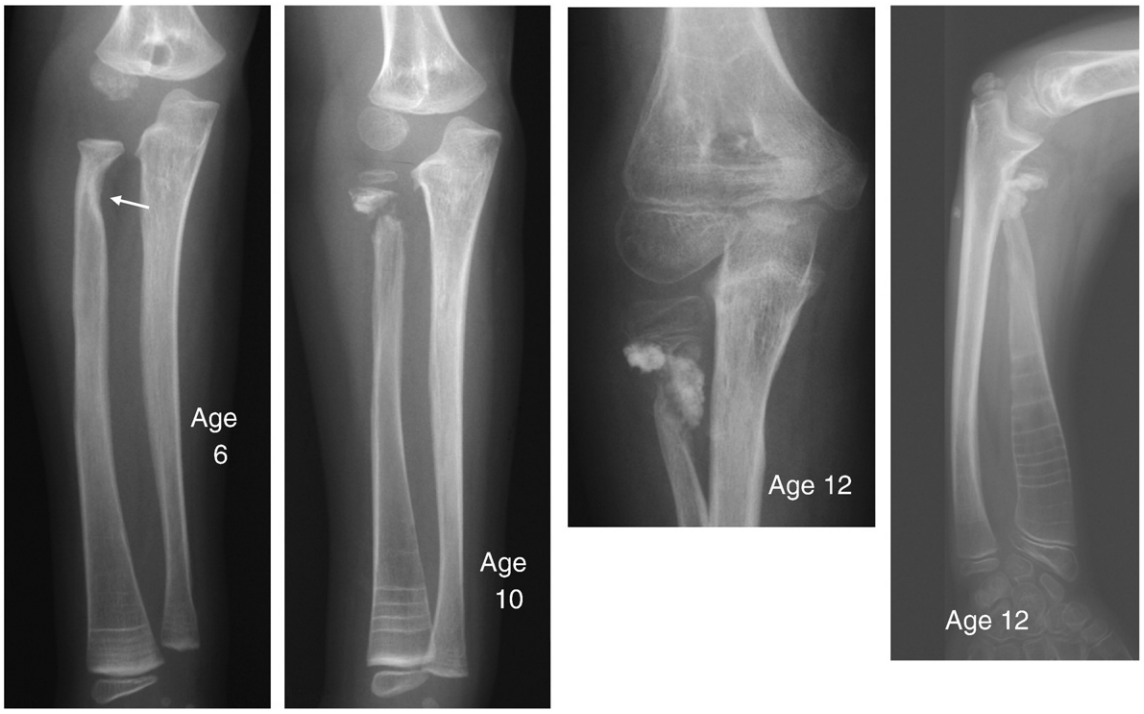

Fig. 4. Submetaphyseal erosion at the proximal end of the radius was first noted age 6 years (far left, arrow). By the age of 10 years, the proximal radius was almost eroded through (center left). An amorphous calcific mass had developed by the age of 12 years (center right). Note the marked thinning of the distal radial cortex with age (right). The horizontal lines reflect intermittent pamidronate treatment. The metaphyseal widening may also be the consequence of bisphosphonate treatment.

There was no convincing evidence that pamidronate treatment arrested acral erosion. Cortical thickness did not increase with treatment, though the rate of loss appeared to accelerate after pamidronate withdrawal. The estimated volumetric BMD of the 3rd lumbar vertebra increased by 50% on pamidronate but fell rapidly after withdrawal of treatment (Fig. 6).

Genetic analysis

Mutational analysis of genomic DNA isolated from leucocytes showed no mutations in the *LMNA* gene, but the patient had heterozygous mutations in *ZMPSTE24*. One was a p.N256S missense mutation (c.794A→G), the other a novel frameshift mutation (p.Y70fs)

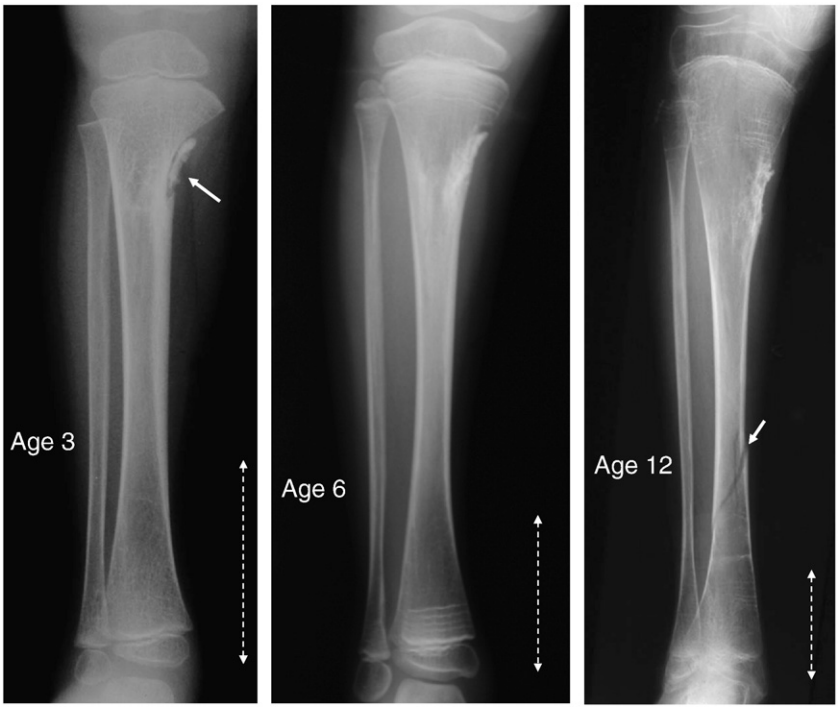

Fig. 5. Submetaphyseal erosion of the medial border of the proximal tibia with an amorphous calcific mass was noted first at the age of 3 (left, arrowed). The appearance was similar at age 6 (center). The horizontal lines in the metaphyses are the consequence of intravenous pamidronate treatment. By the age of 12 years, the cortices had become very thin, and the patient has sustained a spiral fracture (arrow). Over a year later, the fracture had not healed. Arrows with dotted lines indicate 5 cm.

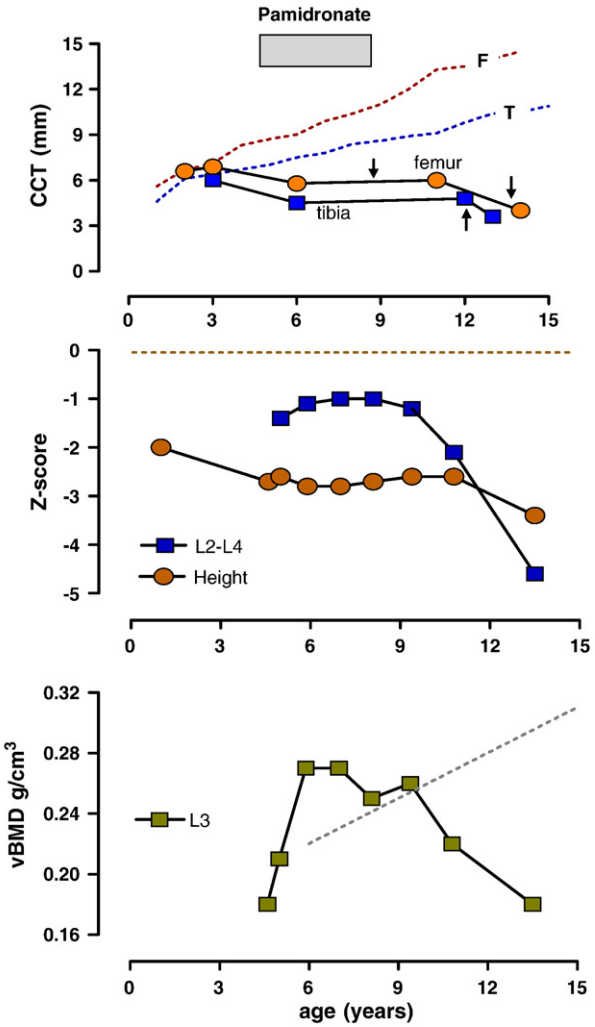

Fig. 6. Top panel: Sequential measurements of combined cortical thickness (CCT) measured at the mid-point of the femur and tibia. The dotted lines indicate mean values in normal subjects. Note the absolute reduction in cortical thickness between the ages of 3 and 14 years.The arrows indicate the timing of fractures of the femur (2) and the tibia. Middle panel: sequential changes in lumbar spine areal BMD and height *z*-scores. Note the dramatic fall in BMD after stopping pamidronate. Lower panel: sequential changes in lumbar spine estimated volumetric BMD. Note the marked improvement with initiation of pamidronate treatment and rapid loss on withdrawal. The dotted line indicates the mean value in normal subjects.

predicted to result in the c.207_208delCT microdeletion in exon 2 (Fig. 7). The patient's mother is an asymptomatic carrier of the missense mutation. The frameshift mutation was not found in blood of the patient's father and non-paternity was excluded. Despite using molecular techniques with a 5% detection rate for germinal mosaicism, we did not find the mutation in a paternal sperm sample, suggesting that the frameshift mutation had arisen *de novo*.

Discussion

MAD type A (MADA) and type B (MADB) are recessively inherited progeroid-like conditions characterized by a range of abnormalities including atrophic skin, lipodystrophy, insulin resistance and metabolic complications. The skeletal phenotype of both diseases, which includes mandibular and clavicular hypoplasia, and acral osteolysis, is distinctive. Our patient with heterozygous mutations in the *ZMPSTE24* gene had several unusual skeletal abnormalities including premature tooth eruption, beaking of the vertebrae, the development of amorphous subcutaneous calcific deposits, progressive submetaphyseal changes at the proximal ends of long bones and severe osteoporosis with fractures and delayed healing.

We reviewed clinical descriptions and radiographs of patients in published reports of MAD with proven *LMNA* or *ZMPSTE24* mutations to establish whether the skeletal phenotype differed. We identified 10 reports describing 25 patients with *LMNA* mutations [13,19–27] and (including the current one) 6 patients with *ZMPSTE24* mutations [14–16,28–31] (some patients have been described more than once at different stages of life). The median age at diagnosis was less in patients with *ZMPSTE24* mutations (~4 months vs. ~4 years for *LMNA* patients), suggesting that the former have a more severe phenotype. Mandibular hypoplasia, dental crowding, clavicular resorption, acral osteolysis and short stature were common to both types, but there were a number of skeletal features more frequently seen in patients with *ZMPSTE24* mutations. These included: premature eruption of primary teeth—67% vs. 4%; amorphous calcific masses—67% vs. 4%; submetaphyseal cortical bone changes—67% vs. 4%; fractures—33% vs. 8% and vertebral beaking—33% vs. 0%. Of the patients with proven *LMNA* mutations, only one subject had amorphous calcific masses, submetaphyseal cortical bone changes and fractures. This was the oldest known surviving MADA subject—a 56-year-old Japanese woman [25]. These findings suggest that patients with MAD due to *ZMPSTE24* mutations have a more severe and "accelerated" skeletal phenotype than those with *LMNA* mutations. Patients with Hutchinson–Gilford progeria syndrome (HGPS) or atypical progeria syndrome (who are heterozygous for *LMNA* mutations) generally have a

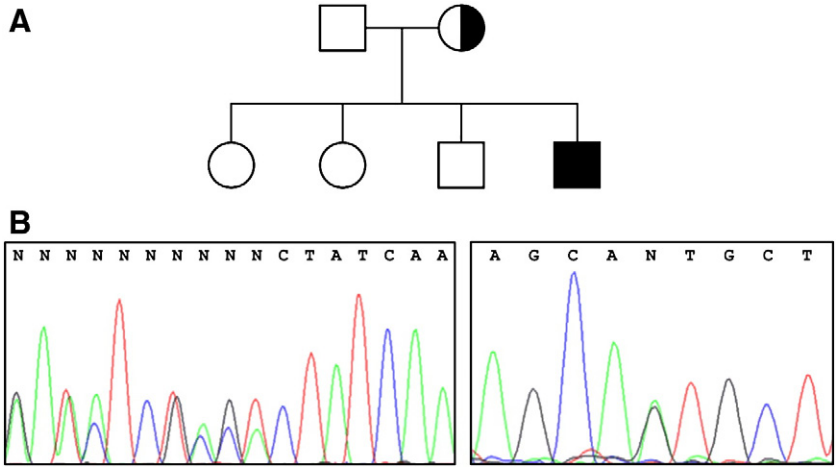

Fig. 7. (A) Pedigree of patient's family. Circles denote female and squares represent males. Filled symbol indicates the proband, half-filled symbol indicates the heterozygote mother and unfilled symbols indicate unaffected family members. (B) Sequence electropherograms showing the missense and frameshift mutations in the *ZMPSTE24* gene.

milder skeletal phenotype than those with MADA (who carry either homozygous or compound heterozygous *LMNA* mutations) [12,32].

A further notable difference in MAD between those with *LMNA* or *ZMPSTE24* mutations was the presence of renal disease in the latter group. Five of the six patients had evidence of renal disease (two with focal segmental glomerulosclerosis who died of renal failure [14,15], two with microhaematuria [16] and our case with proteinuria). Another postulated phenotypic difference is the specific association of *LMNA* mutations with partial lipodystrophy (Type A) and *ZMPSTE24* mutations with generalized lipodystrophy (Type B) [14,16]; however, our case does not support that association. The distinct phenotypic features of MAD with *ZMPSTE24* mutations should lead to future classification according to genotype rather than lipodystrophy pattern.

Zmpste24 knockout mouse models were developed before human mutations were first identified [33,34]. The phenotype included prominent skeletal features such as kyphosis, reduced cortical and trabecular bone mass and fractures [34,35]. Bergo et al. [35] also noted poor healing of fractures, and "pock marks" in long bones in the submetaphyseal zone, reminiscent of the findings we describe here. How the particular skeletal changes of MAD develop is not certain, but *in vitro* lamin A/C knockdown experiments have demonstrated substantially impaired osteoblast proliferation and differentiation, and an increased RANKL/OPG ratio, enhancing osteoclastogenesis [36,37]. In patients with *LMNA* mutations, serum levels of the bone matrix degrading enzyme MMP-9 are increased [38] but the synthesis and mobility of type I collagen by dermal fibroblasts has been reported to be normal [39].

Our patient had a novel truncating mutation (p.Y70fs) in exon 2 of one allele of the *ZMPSTE24* gene, and one previously reported [15,31] missense mutation (p.N256S) in exon 7 of the other allele. Most of the previously reported cases of MAD associated with *ZMPSTE24* mutations have also been heterozygous for one truncating and one missense mutation [14,15,31] but heterozygous missense mutations have also been described [16]. Subjects who are heterozygous for truncating mutations have a normal phenotype, so only one intact copy of *ZMPSTE24* is sufficient. Because of the allele with the missense mutation patients with MAD do retain some, but reduced, enzyme activity, hence their survival. In contrast, inheriting two truncating mutations causes the *in utero* lethal syndrome of restrictive dermopathy [40].

Normal prelamin A contains a CaaX-terminal motif that is a specific target for farnesyl transferase. Farnesylation at this site allows the insertion of the farnesyl group into the cytosolic leaflet of the endoplasmic reticulum membrane [40]. Farnesylation is a prerequisite for the first aaX cleavage by ZMPSTE24. In the absence of ZMPSTE24, the removal of the farnesylated −aaX cannot occur, so prelamin A remains farnesylated and anchored in the membrane. It seems likely that the retention of unprocessed farnesylated prelamin A in the nucleus is toxic to cells, perturbing the recruitment of DNA repair factors to sites of damage [41]. Reducing the accumulation of farnesylated prelamin A has therefore been considered a potential therapeutic strategy. Remarkably, the use of high-dose statins and aminobisphosphonates (which target two enzymes in the farnesyl synthetic pathway, HMG-CoA reductase and Farnesyl-PP synthase, respectively) can almost completely abrogate the phenotype of *Zmpste24* knockout mice [42].

The aminobisphosphonate pamidronate was prescribed to our patient initially in an attempt to limit acral bone resorption. There was little convincing evidence that it was effective in this regard, perhaps because treatment was started too late—the clavicles had already disappeared by the age of 4 years when treatment was begun. However, there was some evidence of a positive effect on bone: the estimated volumetric vertebral bone density increased substantially from values that were subnormal to supranormal for age and fell rapidly on withdrawal of treatment. Despite this, cortical bone was lost and long bone fractures occurred. The poor healing of his first fracture may have been related to recent pamidronate treatment, but subsequent fractures, occurring up to 5 years after withdrawal of treatment, were also very slow to heal. Other patients with MAD have been reported to have osteopenia [20], osteoporosis [16,25] and fractures [16,25,26]; however, delayed healing, as seen in our case, has not been previously reported. Given the success of the high-dose statin and aminobisphosphonate treatment in the *Zmpste24* knockout mouse [42], could this strategy be attempted in future human cases? The doses of pravastatin and zoledronate used in the animal model were ~2 orders of magnitude greater than that which have been used to date in children, so it would be high risk, given the problems with delayed healing after osteotomy and inhibition of metaphyseal remodeling that have emerged with intensive bisphosphonate therapy [43–45]. Osteonecrosis of the jaw has not been seen in children treated with conventional doses of bisphosphonates but could be a concern if greatly increased doses were used. Recently, pharmacological protocols to treat HGPS and MADA patients with a combination of statins and aminobisphosphonates alone or in addition to farnesyltransferase inhibitors (FTIs) have been developed. A phase II open trial for progeria using a combination of zoledronate and pravastatin has started in France, and in Italy, a MADA clinical trial, based on the French protocol, has been approved by Italian Drug Agency (project FARM7XE439) is currently recruiting patients.

Acknowledgments

We thank the late Dr. Alan Parsons for all his care and dedication in this boy's early care, Dr. Salim Aftimos and Dr. Paul Hofman for their support and advice and Dr. Jeremy Clarkson who assisted in preparation of this report.

References

[1] Walton NP, Brammar TJ, Coleman NP. The musculoskeletal manifestations of Werner's syndrome. J Bone Joint Surg (B) 2000;82:885–8.
[2] Shiraki M, Aoki C, Goto M. Bone and calcium metabolism in Werner's syndrome. Endocr J 1998;45:505–12.
[3] German J. Bloom's syndrome. Dermatol Clin 1995;13:7–18.
[4] Mehollin-Ray AR, Kozinetz CA, Schlesinger AE, Guillerman RP, Wang LL. Radiographic abnormalities in Rothmund-Thomson syndrome and genotype-phenotype correlation with RECQL4 mutation status. AJR Am J Roentgen 2008;191:W62–6.
[5] Pasquier L, Laugel V, Lazaro L, Dollfus H, Journel H, Edery P, et al. Wide clinical variability among 13 new Cockayne syndrome cases confirmed by biochemical assays. Arch Dis Child 2006;91:178–82.
[6] Niedernhofer LJ, Garinis GA, Raams A, Lalai AS, Robinson AR, Appeldoorn E, et al . Hoeijmakers JHJ.A new progeroid syndrome reveals that genotoxic stress suppresses the somatotroph axis. Nature 2006;444:1038–43.
[7] Faghri S, Tamura D, Kraemer KH, Digiovanna JJ. Trichothiodystrophy: a systematic review of 112 published cases characterises a wide spectrum of clinical manifestations. J Med Genet 2008;45:609–21.
[8] Hennies HC, Kornak U, Zhang H, Egerer J, Zhang X, Seifert W, et al. Gerodermia osteodysplastica is caused by mutations in SCYL1BP1, a Rab-6 interacting golgin. Nat Genet 2008;40:1410–2.
[9] Reversade B, Escande-Beillard N, Dimopoulou A, Fischer B, Chng SC LiY, Shboul M, et al. Mutations in PYCR1 cause cutis laxa with progeroid features. Nat Genet 2009;41:1016–21.
[10] David LR, Finlon M, Genecov D, Argenta LC. Hallermann-Streiff syndrome: experience with 15 patients and review of the literature. J Craniofac Surg 1999;10:160–8.
[11] Arboleda H, Quintero L, Yunis E. Wiedemann-Rautenstrauch neonatal progeroid syndrome: report of three new patients. J Med Genet 1997;34:433–7.
[12] Merideth MA, Gordon LB, Clauss S, Sachdev V, Smith ACM, Perry MB, et al. Phenotype and course of Hutchinson–Gilford progeria syndrome. N Eng J Med 2008;358:592–604.
[13] Novelli G, Muchir A, Sangiuolo F, Helbling-Leclerc A, D'Apice MR, Massart M, et al. Mandibuloacral dysplasia is caused by a mutation in LMNA-encoding lamin A/C. Am J Hum Genet 2002;71:426–31.
[14] Agarwal AK, Fryns JP, Auchus RJ, Garg A. Zinc metalloproteinase, ZMPSTE24, is mutated in mandibuloacral dysplasia. Hum Mol Genet 2003;12:1995–2001.
[15] Agarwal AK, Zhou XJ, Hall RK, Nicholls K, Bankier A, Van Esch H, et al. Focal segmental glomerulosclerosis in patients with mandibuloacral dysplasia owing to ZMPSTE24 deficiency. J Investig Med 2006;54:208–13.
[16] Miyoshi Y, Akagi M, Agarwal AK, Namba N, Kato-Nishimura K, Mohri I, et al. Severe mandibuloacral dysplasia caused by novel compound heterozygous ZMPSTE24 mutations in two Japanese siblings. Clin Genet 2008;73:535–44.
[17] Carter DR, Bouxsien ML, Marcus R. New approaches for interpreting projected bone densitometry data. J Bone Miner Res 1992;7:137–45.

[18] Virtama P, Helela T. Radiographic measurements of cortical bone. Acta Radiol 1969;293:6–268 supp.
[19] Simha V, Agarwal AK, Oral EA, Fryns JP, Garg A. Genetic and phenotypic heterogeneity in patients with mandibuloacral dysplasia-associated lipodystrophy. J Clin Endocrinol Metab 2003;88:2821–4.
[20] Shen JJ, Brown CA, Lupski JR, Potocki L. Mandibuloacral dysplasia caused by homozygosity for the R527H mutation in lamin A/C. J Med Genet 2003;40:854–7.
[21] Plasilova M, Chattopadhyay C, Pal P, Schaub NA, Buechner SA, Mueller HJ, et al . Homozygous missense mutation in the lamin A/C gene causes autosomal recessive Hutchinson–Gilford progeria syndrome. J Med Genet 2004;41:609–14.
[22] Garg A, Cogulu O, Ozkinay F, Onay H, Agarwal AK. A novel homozygous Ala529Val LMNA mutation in Turkish patients with mandibuloacral dysplasia. J Clin Endocrinol Metab 2005;90:5259–64.
[23] Verstraeten VLRM, Broers JLV, van Steensel MAM, Zinn-Justin S, Ramaekers FCS, Steijlen PM, et al. Compound heterozygosity for mutations in LMNA causes a progeria syndrome without prelamin A accumulation. Hum Mol Genet 2006;15:2509–22.
[24] Lombardi F, Gullotta F, Columbaro M, Filareto A, D'Adamo M, Vielle A, et al. Compound heterozygosity for mutations in LMNA in a patient with a myopathic and lipodystrophic mandibuloacral dysplasia type A phenotype. J Clin Endocrinol Metab 2007;92:4467–71.
[25] Kosho T, Takahashi J, Momose T, Nakamura A, Sakurai A, Wada T, et al. Mandibuloacral dysplasia and a novel LMNA mutation in a woman with severe progressive skeletal changes. Am J Med Genet 2007;143A:2598–603.
[26] Agarwal AK, Kazachkova I, Ten S, Garg A. Severe mandibuloacral dysplasia-associated lipodystrophy and progeria in a young girl with a novel homozygous Arg527Cys LMNA mutation. J Clin Endocrinol Metab 2008;93:4617–23.
[27] Garavelli L, D'Apice MR Rivieri F, Bertoli M, Wischmeijer A, Gelmini C, De Nigris V, et al. Mandibuloacral dysplasia type A in childhood. Am J Med Genet 2009;149A: 2258–64.
[28] Schrander-Stumpel C, Spaepen A, Fryns JP, Dumon J. A severe case of mandibuloacral dysplasia in a girl. Am J Med Genet 1992;43:877–81.
[29] Pedagogos E, Flanagan G, Francis DMA, Becker GJ, Danks DM, Walker RG. A case of craniomandibular dermatodysostosis associated with focal glomerulosclerosis. Pediatr Nephrol 1995;9:354–6.
[30] Danks DM, Mayne V, Norman H, Wettenhall B, Hall RK. Craniomandibular dermatodysostosis. Birth Defects 1974;10:99–105.
[31] Shackleton S, Smallwood DT, Clayton P, Wilson LC, Agarwal AK, Garg A, et al. Compound heterozygous ZMPSTE24 mutations reduce prelamin A processing and result in a severe progeroid phenotype. J Med Genet 2005;42:e36.
[32] Garg A, Subramanyam L, Agarwal AK, Simha V, Levine B, D'Apice MR, et al. Atypical progeroid syndrome due to heterozygous missense LMNA mutations. J Clin Endocrinol Metab 2009;94:4971–83.
[33] Leung GK, Schmidt WK, Bergo MO, Gavino B, Wong DH, Tam A, et al. Biochemical studies of Zmpste24-deficient mice. J Biol Chem 2001;276:29051–8.
[34] Pendás AM, Zhou Z, Cadiñanos J, Freije JM, Wang J, Hultenby K, et al. Defective prelamin A processing and muscular and adipocyte alterations in Zmpste24 metalloproteinase-deficient mice. Nat Genet 2002;31:94–9.
[35] Bergo MO, Gavino B, Ross J, Schmidt WK, Hong C, Kendall LV, et al. Zmpste24 deficiency in mice causes spontaneous bone fractures, muscle weakness, and a prelamin A processing defect. Proc Nat Acad Sci 2002;99:13049–54.
[36] Akter R, Rivas D, Geneau G, Drissi H, Duque G. Effect of lamin A/C knockdown on osteoblast differentiation and function. J Bone Miner Res 2009;24:283–93.
[37] Rauner M, Sipos W, Goettsch C, Wutzl A, Foisner R, Pietschmann P, et al. Inhibition of lamin A/C attenuates osteoblast differentiation and enhances RANKL-dependent osteoclastogenesis. J Bone Miner Res 2009;24:78–86.
[38] Lombardi F, Fasciglione GF, D'Apice MR, Vielle A, D'Adamo M, Sbraccia P, et al. Increased release and activity of matrix metalloproteinase-9 in patients with mandibuloacral dysplasia type A, a rare premature ageing syndrome. Clin Genet 2008;74:374–83.
[39] Nguyen D, Leistritz DF, Turner L, MacGregor D, Ohson K, Dancey P, et al . Collagen expression in fibroblasts with a novel LMNA mutation. Biochem Biophys Res Comm 2007;352:603–8.
[40] Navarro C, Cau P, Levy N. The molecular basis of progeroid syndromes. Hum Mol Genet 2006;15(review issue 2):R151–61.
[41] Liu B, Wang J, Chan KM, Tjia WM, Deng W, Guan X, et al. Genomic instability in laminopathy-based premature aging. Nat Med 2005;11:780–5.
[42] Varela I, Pereira S, Ugalde AP, Navarro CL, Suárez MF, Cau P, et al. Combined treatment with statins and aminobisphosphonates extends longevity in a mouse model of human premature aging. Nat Med 2008;14:767–72.
[43] Munns CF, Rauch F, Zeitlin L, Fassier F, Glorieux FH. Delayed osteotomy but not fracture healing in pediatric osteogenesis imperfecta patients receiving pamidronate. J Bone Miner Res 2004;19:1779–86.
[44] Whyte MP, Wenkert D, Clements KL, McAlister WH, Mumm S. Bisphosphonate-induced osteopetrosis. N Eng J Med 2003;349:455–61.
[45] Whyte MP, McAlister WH, Novack DV, Clements KL, Schoenecker PL, Wenkert D. Bisphosphonate-induced osteopetrosis: novel bone modeling defects, metaphyseal osteopenia, and osteosclerosis fractures after drug exposure ceases. J Bone Miner Res 2008;23:1698–707.